Modulation of Atherothrombotic Factors: Novel Strategies for Plaque Stabilization

Bot, I.

6

Adventitial Mast Cell Activation Causes Atherosclerotic Plaque Destabilization in ApoE$^{-/-}$ mice

*Ilze Bot, *Saskia C.A. de Jager, Bernard A. Slütter, Bianca C.H. Lutters, Theo J.C. van Berkel, Erik A.L. Biessen

*both authors contributed equally to this study

Division of Biopharmaceutics, Leiden/Amsterdam Center for Drug Research, Leiden University, Leiden, The Netherlands.

Submitted

Abstract

While activated mast cells have been found to be abundantly present in the adventitia of ruptured atherosclerotic plaques, it remains unclear whether their presence is a mere epiphenomenon or causal to the pathobiology. In this study, we activated mast cells in the adventitia of advanced carotid artery plaques of ApoE$^{-/-}$ mice and addressed their effect on plaque phenotype. The increased mast cell degranulation translated into a dramatically increased incidence of intraplaque hemorrhage, which was found to be accompanied by H_1-receptor and mast cell protease-dependent macrophage apoptosis and partly by enhanced vascular leakage and *de novo* leukocyte recruitment to the plaque. Importantly, treatment with mast cell stabilizer cromolyn normalized degranulated mast cell levels and prevented hemorrhage. These data imply that activated mast cells play a significant role in plaque destabilization and we propose that mast cell stabilization could be an effective new therapeutic entry in the prevention of acute coronary syndromes.

Introduction

Acute coronary syndromes including unstable angina and myocardial infarction are commonly caused by erosion or rupture of vulnerable atherosclerotic plaques, which are characterized by a large lipid core covered by a thin fibrous cap[1,2,3]. Inflammatory cells are considered to play a key role in the pathogenesis of plaque rupture[4,5,6]. One of the inflammatory cell types, the mast cell[7], has been shown to accumulate in the rupture-prone shoulder region of human atheromas[8]. Activated mast cells containing proteases such as tryptase and chymase, have been identified at the site of atheromatous erosion or rupture in specimens of human coronary arteries[9]. These mast cell proteases are known to activate matrix-metalloproteases (MMPs)[10] and to induce apoptosis of vascular smooth muscle cells[11]. Human coronary artery specimens contain TNFα-rich activated mast cells[12,13], which potentially aggravates the ongoing inflammatory response and also induce the production of gelatinase (i.e. MMP-9) by macrophages. These processes can ultimately lead to plaque destabilization. Not only intimal inflammation but also inflammation of the arterial adventitia has been shown to influence the vulnerability of the plaque[14]. Recently, activated mast cells have been identified in the adventitia of vulnerable and ruptured lesions in patients with myocardial infarction[15-17] and more importantly, their number was found to correlate with the incidence of plaque rupture and erosion[15]. In these studies, it is suggested that histamine released from adventitial mast cells might trigger plaque rupture. However, it remains to be clarified whether adventitial mast cells are instrumental in plaque rupture or should be considered to be attracted secondary to the process. In this study, we have recruited mast cells to the adventitia of atherosclerotic carotid artery lesions of ApoE$^{-/-}$ mice and activated them via a novel sensitization/local challenge protocol and we demonstrate that this recruitment and activation of mast cells promotes macrophage apoptosis and microvascular leakage and importantly, enhances the incidence of intraplaque hemorrhage. Furthermore, mast cell stabilization by cromolyn does prevent these pathophysiological events by inhibition of mast cell degranulation in the adventitia of these atherosclerotic plaques.

Methods

Animals

All animal work was performed in compliance with the Dutch government guidelines. Male ApoE$^{-/-}$ mice, obtained from the local animal breeding facility, were fed a Western type diet, containing 0.25% cholesterol and 15% cacaobutter (SDS, Sussex, UK). Atherosclerotic carotid artery lesion formation was induced by perivascular collar placement as described previously[18]. Mice were anaesthetized by subcutaneous injection of ketamine (60 mg/kg, Eurovet Animal Health, Bladel, The Netherlands),

fentanyl citrate and fluanisone (1.26 mg/kg and 2 mg/kg respectively, Janssen Animal Health, Sauderton, UK). Five weeks after collar placement all animals were skin-sensitized as described by Kraneveld *et al*.[19]. In short, on day 1 and 2 isoflurane anaesthetized mice received either DNFB (0.5% v/v, Janssen Chimica, Beerse, Belgium, n=12) or vehicle solution (acetone:olive oil 4:1, n=14). On day 5, the mice were challenged perivascularly by applying pluronic F-127 gel (25% w/v) or pluronic F-127 gel containing DNP (50 µg/animal) at the lesion site. To measure *de novo* infiltration of circulating leukocytes into the lesions, some of the mice were injected intravenously with Rhodamine 6G (0.67 mg/kg)[20] to label circulating leukocytes. In a separate experimental set-up, two groups of mice (control: n=6 and DNFB sensitized: n=4) received an intravenous injection containing 25 mg/kg of the mast cell stabilizer cromolyn (Sigma, Zwijndrecht, The Netherlands)[21,22] thirty minutes before local challenge and twice daily during challenge by intraperitoneal injections with 50 mg/kg of cromolyn.
The mouse Mast Cell Proteases (mMCP) and TNFα levels in plasma were determined by commercially available ELISAs (Moredun Scientific Ltd., Midlothian, Scotland and BD BioSciences, San Diego, USA, respectively). Three days after challenge the animals were anaesthetized and *in situ* fixation through the left cardiac was performed[18].

Histology
Mast cells were visualized by staining of 5 µm cryosections with aqueous toluidin blue (Sigma) and by chloroacetate esterase (CAE) reactivity, while mast cell phenotype was established using an Alcian Blue/Safranin O staining (Sigma). An iron staining was performed according to Perl's method. Endothelium was stained by use a CD31 monoclonal antibody (BD BioSciences), while apoptosis was visualized using a terminal deoxytransferase dUTP nick-end labeling (TUNEL) kit (Roche Diagnostics).

Morphometry
Morphometric analysis (Leica Qwin image analysis software) was performed on hematoxylin-eosin stained sections of the carotid arteries at the site of maximal stenosis[18]. Toluidin blue stained sections were used for histological examination for the presence of adventitial mast cells. Mast cells numbers, the extent of mast cell degranulation and presence of iron were assessed manually. TUNEL positive areas were quantified both by Leica Qwin image analysis software and by manual counting of TUNEL positive nuclei. All morphometric analyses were performed by a blinded independent operator.

Cell culture
MC/9 cells, kindly provided by Dr. Renauld from the Ludwig Institute for Cancer Research in Belgium, were cultured as described previously[23]. MC/9 cells ($2.5*10^5$) were degranulated by incubation with 0.5 µg/mL of compound 48/80 (Sigma) for 15 minutes at 37°C. Cells were centrifuged (1,500 rpm, 5 minutes) and the supernatant was used for further experiments.

Apoptosis assay
VSMCs were obtained from thoracic aortas from male C57Bl/6 mice using collagenase digestion and cultured as previously described[24]. The murine macrophage cell line RAW 264.7 was cultured in DMEM containing 10% FBS, 2 mmol/L L-glutamine, 100 U/mL penicillin and 100 µg/mL streptomycin (all from Cambrex, Verviers, Belgium). VSMCs and RAW 264.7 cells were seeded at a density of 10^5 cells/cm^2 and exposed to supernatant from degranulated and undegranulated MC/9 cells for 24 hours (RAWs) or for 48 and 72 hours (vSMCs) after which cellular DNA was stained with propidium iodide (Sigma). The effect of mast cell chymase and tryptase inhibition on apoptosis was determined using the soybean trypsin inhibitor and leupeptin (both 100 mg/L, Sigma)[25], while the involvement of histamine receptors in apoptosis was addressed by measuring apoptosis in the presence of the H_1-, H_2- and H_3-receptor antagonists triprolide (1 µM), cimetidine (100 µM) and thioperamide (1 µM, all from Sigma)[26] respectively. Also, the effect of single mast cell compounds was addressed using 35 mM of histamine and 500 U/L tryptase (both from Sigma). Cells were preincubated with either histamine or tryptase for 16 hours and after removal of this medium, the macrophages were incubated with either tryptase or histamine for an additional 6 hours, after which apoptosis was measured. DNA fragmentation was measured using FACS analysis (FACScalibur, BD Biosciences).

Clot assay
Mouse plasma was obtained by orbital bleeding in 3.8% (w/v) citrate and centrifugation at 5,000 rpm for 5 minutes. MC/9 cells ($2.5*10^5$ cells/mL) were degranulated at 37°C for 30 minutes in HEPES buffer containing 100 ng/mL DNP. The clot lysis assay was performed as described by Lisman *et al*.[27], without addition of tPA to avoid impaired clotting of mouse plasma.

Microvascular leakage
Increased microvascular permeability was assessed essentially as described by Sirois *et al*.[28] and Walls *et al*.[29] with minor modifications. In short, male C57Bl/6 mice were injected intradermally at randomized sites with either $5*10^5$ MC/9 mast cells suspended in PBS containing 50 µg/mL compound 48/80 in the absence or presence of histamine receptor antagonists (0.1 mM triprolidine, 10 mM cimetidine or 0.1 mM thioperamide) or chymase and tryptase inhibitors (10 g/L SBTI or leupeptin, respectively). Immediately after

intradermal injection of the cell suspensions, 100 µL 1.25% Evans Blue was injected intravenously and after 30 minutes, the surface area of Evans Blue stained skin was measured. To measure *de novo* infiltration of circulating leukocytes into the skin, mice were injected intravenously with Rhodamine 6G (0.67 mg/kg)[20] to label circulating leukocytes, subsequent to intradermal injection with MC/9 mast cells. After 30 minutes, the skin was fixed and cellular infiltrates were scored manually.

Statistical analysis

Data are expressed as mean ± SEM. A 2-tailed Student's t-test was used to compare individual groups. Non-parametric data were analyzed using a Mann-Whitney U test. Frequency data analysis was performed by means of the Fisher's exact test. Matched non-parametric data were analyzed using a Friedman test. A level of $P<0.05$ was considered significant.

Results

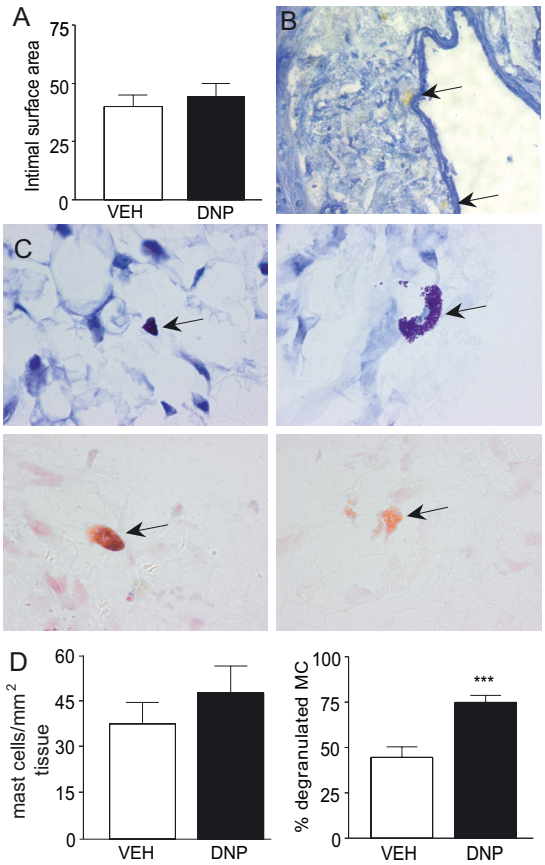

Figure 1. Mast cell content in the adventitia of atherosclerotic lesions. (A) Intimal surface area (*10^3 µm^2) of the control and DNP challenged animals. (B) Atherosclerotic lesion containing intracellular yellow DNP deposits, as indicated by the arrows. (C) Toluidin Blue (upper panels) and Alcian Blue/Safranin O staining (lower panels) of resting (left panels) and activated (degranulating, right panels) mast cells in the adventitia of an atherosclerotic lesion (1000x). (D) Total adventitial mast cell content in control and DNP treated animals (left panel). Adventitial mast cell degranulation in control and DNP challenged mice, which was found to be significantly increased in the latter group (***P=0.0005, right panel).

Dinitrophenyl albumin challenge

To recruit mast cells to the adventitia of carotid artery plaques we adapted the conventional dinitrophenyl albumin (DNP) sensitization/challenge protocol by use of a DNP loaded pluronic F-127 gel, which was applied perivascularly at the lesion site. First, we studied the kinetics of DNP release from this gel *in vitro* at 37°C. Almost 50% of the incorporated DNP was released within 1 hr, while after 6 hrs DNP was almost completely diffused from the gel regardless of the initial DNP concentration (data not shown). To induce local mast cell activation *in vivo*, $ApoE^{-/-}$ mice were perivascularly challenged at the site of collar-induced carotid artery atherosclerotic lesions[18]. Plasma mouse Mast Cell Protease (mMCP) levels did not differ between control and DNP challenged animals (6.45 ± 0.92 ng/mL versus 7.15 ± 0.84 ng/mL, respectively) three days after challenge. Likewise, plasma TNFα levels were essentially similar in the control and DNP challenged group (55.8 ± 1.9 pg/mL and 64.3 ± 5.5 pg/mL, respectively, P=0.17), suggesting that the challenge protocol did not result in systemic mast cell degranulation.

Adventitial mast cells and plaque morphology

The sensitization/challenge protocol did not affect body weight and plasma total cholesterol levels of Western type diet fed $ApoE^{-/-}$ mice throughout the study (data not shown). Morphometric analysis of carotid artery lesions did not reveal any differences in plaque size between control and DNP challenged animals ($40 \pm 5*10^3$ μm^2 versus $44 \pm 6*10^3$ μm^2 respectively, Figure 1A). Medial size was slightly but significantly increased in the DNP challenged mice ($28 \pm 3*10^3$ μm^2 versus $23 \pm 2*10^3$ μm^2 in the control group, P=0.04). Intracellular DNP granules were detected in the central atheroma of the lesions, illustrating not only the effective DNP release from the gel, but also the dynamics of the advanced plaque (Figure 1B). Resting and activated mast cells in the adventitia of the lesions were firmly established by toluidin blue (Figure 1C), chloroacetate esterase (CAE) and Alcian Blue/Saphranin O. Alcian Blue/Saphranin O staining (Figure 1C) of the adventitial mast cells revealed that the vast majority (98.6%) were connective tissue-type mast cells[30].

While the absolute number of adventitial mast cells in the toluidin blue stained sections did not differ three days after perivascular challenge ($4.8 \pm 1.3*10^{-5}$ versus $3.8 \pm 1.2*10^{-5}$ MC/μm^2 adventitial tissue in the controls, P=0.3), the percentage of degranulated mast cells after DNP challenge was found to be significantly increased (74.7 ± 3.9% versus 44.6 ± 5.8% in control animals, P=0.0005, Figure 1D). The cell density of the adventitia of DNP challenged animals tended to be higher ($4.8 \pm 0.7*10^{-3}$ cells/μm^2 adventitial tissue) compared to vehicle treated control animals ($3.7 \pm 0.5*10^{-3}$ cells/μm^2 adventitial tissue, P=0.08).

Strikingly, further analysis of the plaque morphology three days after challenge revealed intraplaque hemorrhages in 7 of 24 plaques of DNP challenged animals (Figure 2A) while we observed no such phenomena in control plaques (Figure 2D, 0 of 28, P=0.003). These lesions contained high erythrocyte numbers (Figure 2B) and in the near proximity of hemorrhages, CD31 positive microvessels were detected (Figure 2C). To exclude the possibility that these events represented perfusion or isolation artefacts, we performed a Perl's Iron staining, showing an equally strong increase in iron positive sections for DNP challenged animals (6 of 24 compared to 0 of 28 for control mice, Figures 2E to G; P=0.007). Iron staining was found to correlate with the presence of intraplaque hemorrhage (P<0.0001), co-localized with ceroid-rich regions and was confined mostly to the central atheroma. Of 6 lesions with Iron positive intima's, 5 arteries revealed Iron staining also in the media (P=0.02) and enhanced medial thickening.
As mast cell degranulation was reported to promote apoptosis of vSMCs and EC[11,31,32], thus affecting plaque stability, we stained sections for apoptotic cells by TUNEL staining (Figure 3A). Indeed, we observed a significant increase in TUNEL positive area in DNP challenged lesions (3.3 ± 0.5% TUNEL stained area compared to 0.6 ± 0.2% in the control, P=0.003, Figure 3B), which was confirmed by blinded scoring of the TUNEL positive nuclei in the plaque (6.1 ± 2.0% versus 2.1 ± 0.6% in the controls, P=0.002). While the iron negative lesions of the DNP challenged animals displayed enhanced levels of TUNEL positive nuclei (2.6 ± 0.6% TUNEL positive area, P=0.02 compared to controls), the degree of apoptosis was even more pronounced in the iron positive sections (4.8 ± 0.6% TUNEL positive area, P=0.01). Surprisingly, the majority of the apoptotic cells was located in the central atheroma rather than in the SMC rich cap of the lesions (P=0.04, Figure 3C), implying that mast cell degranulation preferentially induces macrophage apoptosis.

MC/9 cell degranulation induces apoptosis of macrophages
Supernatant from IL-3 stimulated MC/9 mast cells, which were degranulated with compound 48/80, induced apoptosis of RAW 264.7 macrophages in a concentration dependent manner up to 5-fold (21.8 ± 0.7% of apoptotic cells compared to 4.4 ± 0.3% in the control, Figure 4A). To pinpoint the actual mast cell constituent that is responsible for macrophage apoptosis, we assessed the effect of tryptase (leupeptin), chymase (SBTI) inhibitors as well as of histamine receptor antagonists on mast cell-induced apoptosis. Both SBTI (100 mg/L) and leupeptin (100 mg/L) were able to completely prevent the mast cell-induced apoptosis. Similarly, the H_1-receptor antagonist triprolidine (1 µM) inhibited the mast cell induced apoptosis of macrophages, while the H_2- and H_3-receptor antagonists cimetidine (100 µM) and thioperamide (1 µM) were ineffective (Figure 4A).

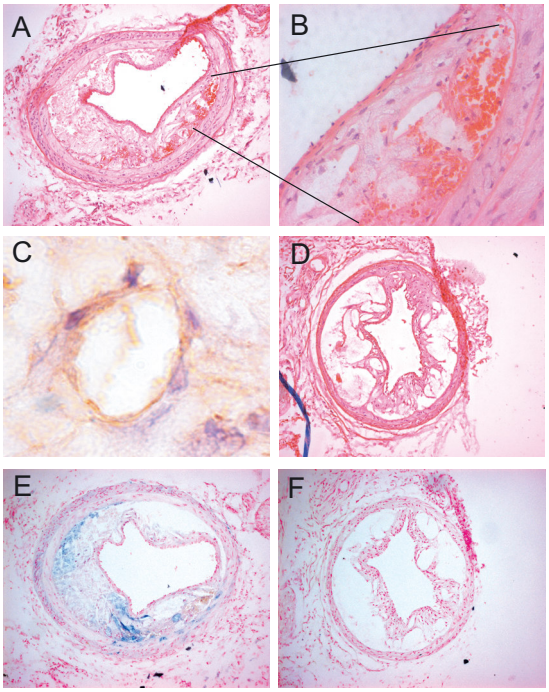

G

Events	+	-	Total
Control	0	26	26
DNP	7	17	24

Iron	+	-	Total
Control	0	26	26
DNP	6	18	24

Figure 2. Increased incidence of intra-plaque hemorrhage in DNP challenged animals. (A) Hematoxylin/Eosin staining of a plaque from a DNP challenged mouse (100x), demonstrating intra-plaque hemorrhages (B, 1000x) and neovascularization (C, 1000x), confirmed by a CD31 staining. (D) Hematoxylin/Eosin staining of a control plaque. (E,F) Perl´s iron staining of a DNP (E) and a vehicle control challenged artery (F), revealing large areas with iron deposits only in the DNP challenged plaque (100x). (G) Quantification of the number of plaques containing hemorrhages and iron deposits in vehicle and DNP challenged mice, establishing a strongly increased frequency of hemorrhages after DNP challenge (**P=0.003), which was confirmed by Perl's iron staining (*P=0.007).

None of the inhibitors affected H_2O_2 induced apoptosis of RAW 264.7 cells, thus excluding that the used inhibitors are anti-apoptotic by themselves (data not shown). As both the protease inhibitors as the H_1-receptor antagonist are able to completely inhibit the mast cell induced apoptosis, we verified whether histamine acts synergistically on tryptase induced macrophage apoptosis or vice versa. Incubation with histamine for 16 hours strongly induced macrophage apoptosis (9-fold, $P<0.01$), while subsequent post-treatment with tryptase (6 hours) led to an additive (1.8-fold) increase in macrophage apoptosis compared to treatment with histamine only. Tryptase treatment for 6 hours appeared to be ineffective. Conversely, priming of macrophages with tryptase for 16 hours slightly enhanced RAW 264.7 cell apoptosis (13 ± 3% compared to 4 ± 2% for untreated cells, $P=0.05$), but did not sensitize macrophages for histamine induced apoptosis (data not shown). In agreement with other studies, supernatant of degranulated mast cells induced vSMC apoptosis after 48 hours (data not shown), although vSMC appeared to be less susceptible to mast cell induced apoptosis than macrophages.

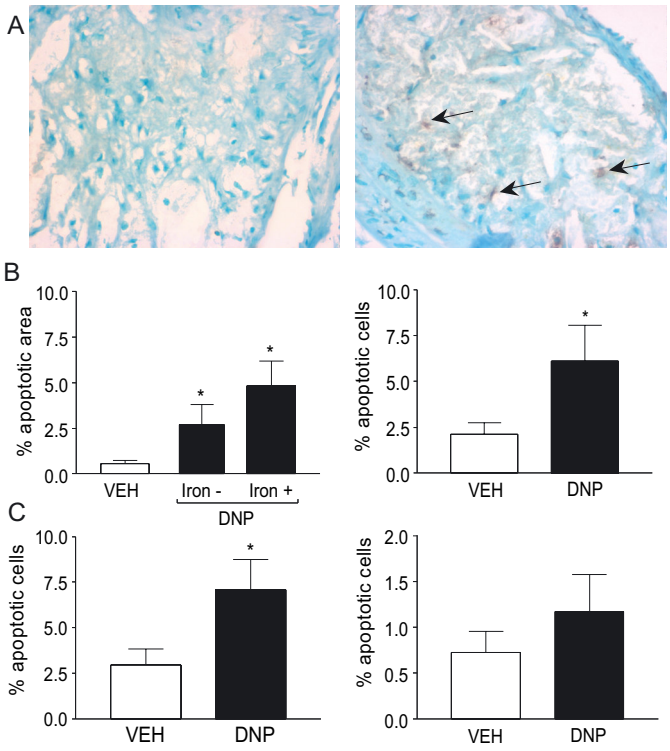

Figure 3. Increased apoptosis in lesions of DNP challenged mice. (A) TUNEL staining of a vehicle (left panel) and a DNP (right panel) challenged artery; arrows indicate TUNEL positive nuclei in brown (200x). (B) Relative TUNEL positive intimal area (left panel) of control, Iron negative and Iron positive DNP challenged plaques, which both showed increased apoptosis in DNP challenged plaques. The percentage of intimal TUNEL positive nuclei of vehicle controls is lower than that of DNP challenged animals (right panel). (C) The percentage of TUNEL positive nuclei was significantly increased in the central core of DNP challenged lesions (left panel), while no significant difference was found in the percentage of TUNEL positive nuclei in the cap region of control and DNP challenged plaques (right panel). *P≤0.05 compared to the control.

Clot assay

Plasma exposed to supernatant of degranulated MC/9 cells displayed a reduced rate of coagulation compared to control medium exposed mouse plasma. The maximal optical density measured after exposure to mast cell supernatant was >50% lower than to the control (Figure 4B), suggestive of a less stable clot due to impaired fibrin formation. Preliminary data suggest that the impaired clot formation was attributable to mast cell tryptase mainly. These data indicate that mast cell constituents, released after degranulation, do not enhance clotting when exposed to clotting factors in the blood circulation.

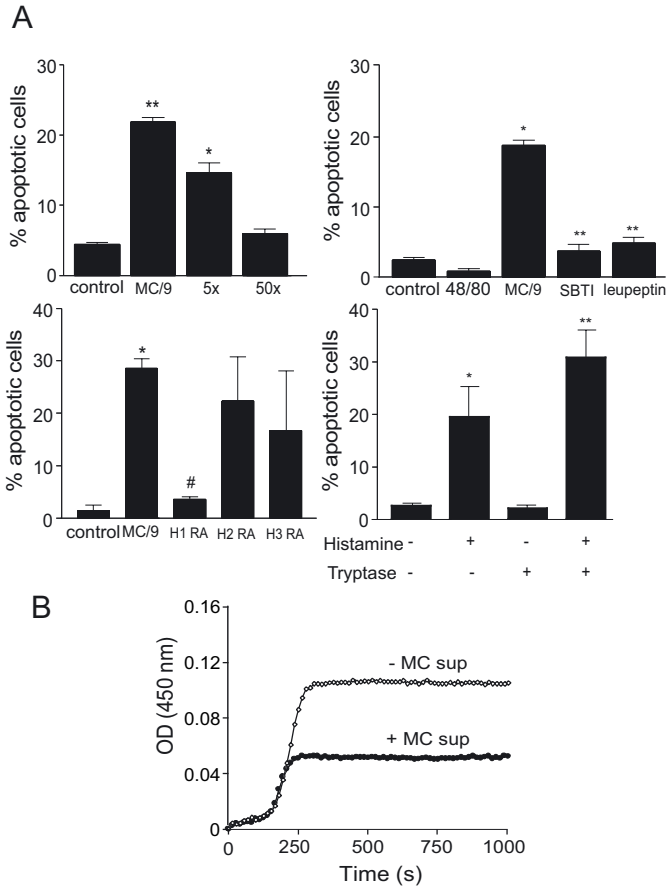

Figure 4. *In vitro* apoptosis of macrophages induced by mast cell degranulation. (A) Supernatant from degranulated murine MC/9 mast cells induced apoptosis of murine RAW 264.7 macrophages in a dose dependent fashion. (*P≤0.05, **P≤0.01 compared to DMEM control, upper left panel). The MC/9 mast cell induced apoptosis of RAW 264.7 cells (*P≤0.05 compared to DMEM control) was inhibited by the chymase inhibitor SBTI and by the tryptase inhibitor leupeptin (**P≤0.01, upper right panel). Compound 48/80, used to degranulate the MC/9 mast cells, did not exert any effect on macrophage apoptosis. Mast cell induced apoptosis was completely abolished by the H_1-receptor antagonist triprolidine ($^{\#}$P≤0.05 compared to the mast cell supernatant induced apoptosis), but not by the H_2-receptor antagonist cimetidine and the H_3-receptor antagonist thioperamide (lower left panel). Incubation of RAW 264.7 cells with 30 mM of histamine induced macrophage apoptosis, which was even enhanced after 6 hour incubation with tryptase, while tryptase itself did not induce apoptosis after 6 hours (lower right panel). (B) Clot lysis curve of mouse plasma exposed to degranulated mast cell supernatant (●), which shows reduced clotting compared to mouse plasma exposed to control buffer (○).

Microvascular leakage study

Apart from promoting macrophage apoptosis, mast cells have been suggested to induce vascular leakage[33,34]. Thirty minutes after intradermal injection of $5*10^5$ MC/9 cells and compound 48/80 in mice, vascular leakage

as judged by the Evans Blue spot size was significantly enhanced as compared to the PBS control (Figure 5A, P<0.001). Enhanced leakage was quenched to control levels by co-injection with the H_1-receptor antagonist triprolidine only (P=0.02), suggesting that the H_1-receptor is primarily responsible for the increased leakage. Injection of compound 48/80 by itself only slightly induced vascular leakage, which can probably be ascribed to degranulation of resident skin mast cells (data not shown). MC/9 cells were also found to orchestrate *de novo* recruitment of leukocytes to the site of injection. Scoring of cellular infiltrates in the injected skin revealed a 1.5- and 8-fold increase in mononuclear cells and neutrophils, respectively, in MC/9 but not PBS control injected skin (both P=0.03, Figure 5B). Increased leukocyte influx was also observed in skin injected with histamine. Upon labelling of circulating leukocytes with Rhodamine 6G prior to skin injections, an increased number of labelled leukocytes were detected in skins injected with MC/9 mast cells (Figures 5C). These data indicate that the observed dermal leukocytes are *de novo* recruited from the circulation due to mast cell induced chemotaxis and enhanced vascular permeability. Also, the total amount of inflammatory cells, not only from the circulation, was increased in the skins injected with activated mast cells or histamine (data not shown). Mice that had been perivascularly challenged with DNP at the carotid artery lesions prior to Rhodamine 6G injection contained a considerably higher number of Rhodamine positive cells (P=0.0002) and also cells per µm intimal surface area (P=0.0009) compared to mock challenged controls (Figure 5D). The Rhodamine positive cells also colocalized with a Hoechst nuclear staining, indicating that the influx we observed are indeed labeled cells (data not shown). Whereas in control mice newly recruited Rhodamine positive leukocytes were mainly found at the plaque surface, in the DNP challenged mice a considerable portion of the Rhodamine positive cells was detected in the central atheroma near the internal elastic lamina, suggesting that the latter had in part migrated through mast cell permeabilized microvessels inside the plaque.

Mast cell stabilization prevents intraplaque hemorrhage

In animals treated with the mast cell stabilizer cromolyn prior to and during challenge, no difference was observed in the total amount of adventitial mast cells between the DNP challenged and control mice ($2.4 \pm 0.8*10^{-5}$ versus $2.1 \pm 0.6*10^{-5}$ per μm^2 adventitial tissue respectively, P=0.8). Cromolyn treatment was also found to normalize the degranulated mast cell content in DNP challenged animals ($47.0 \pm 15.8\%$ versus $40.7 \pm 10.3\%$ for the controls, P=0.4, Figure 6A). More importantly, plaques of cromolyn treated control and DNP challenged mice both did not demonstrate any signs of intraplaque hemorrhage or of intimal or medial Perl's Iron staining (Figure 6B). In analogy to the previous *in vivo* study, we found no differences in plaque size between control and DNP challenged animals ($30 \pm 3*10^5$ μm^2 versus $49 \pm 14*10^5$ μm^2, respectively, P=0.2). Also, medial size did not differ between the groups (data not shown).

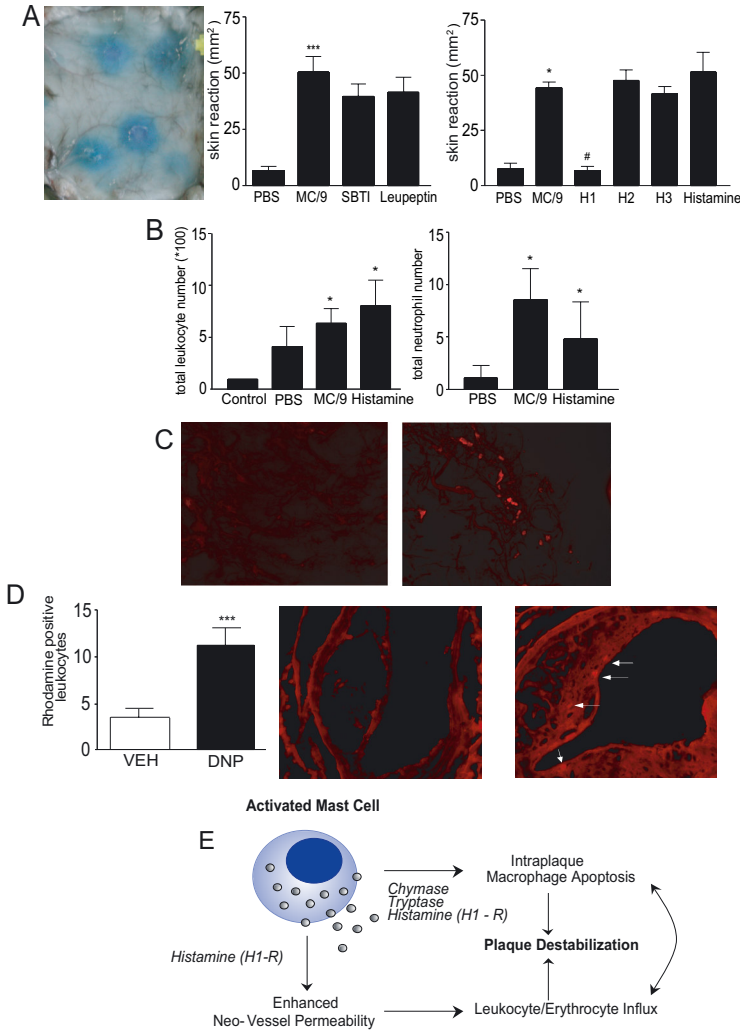

Figure 5. Microvascular leakage was enhanced by degranulated MC/9 mast cells. (A) Evans Blue spots in the skin of C57Bl/6 mice, injected intradermally with degranulating MC/9 mast cells (left panel). Evans Blue stained surface area of MC/9 injected skin was larger than that of PBS control injected skin (***P<0.001) and remained unaffected by co-injection of mast cell protease inhibitors (middle panel). Only co-injection of the H_1-receptor antagonist triprolidine reversed the MC/9 induced vascular leakage (*P<0.05, $^{\#}$P=0.02 compared to the MC/9 cells, right panel). (B) Leukocytes infiltration in the MC/9 injected skin was increased (*P=0.03, left panel). Also, increased neutrophil recruitment was measured in MC/9 or histamine injected skin (*P=0.03, right panel). (C) *De novo* recruitment of circulating Rhodamine 6G labeled leukocytes to the PBS injected skin (400x, left panel). An increased infiltration of Rhodamine 6G labeled leukocytes was observed in skin segments injected with MC/9 mast cells (400x, right panel). (D) Influx of newly recruited leukocytes after *in vivo* labeling with Rhodamine 6G is increased in DNP challenged animals compared to the control animals (***P=0.0002, left panel). The middle and right panels show representative pictures of Rhodamine positive leukocytes, depicted by the white arrows, in control and DNP challenged animals, respectively. (E) Suggested mechanism of adventitial mast cell degranulation on atherosclerotic lesions.

Furthermore, TUNEL staining of lesions from cromolyn treated mice did not reveal any differences between the control and the DNP challenged group (1.5 ± 0.7% versus 2.4 ± 0.9% TUNEL stained area, respectively, P=0.4), suggesting that cromolyn prevented the adventitial mast cell induced apoptosis of macrophages in the central atheroma.

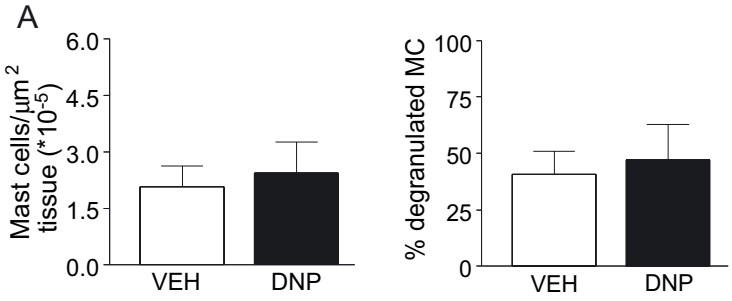

B

Events	+	-	Total
Control	0	14	14
DNP	0	8	8

Iron	+	-	Total
Control	0	10	10
DNP	0	8	8

Figure 6. Cromolyn treatment prevents mast cell induced intraplaque hemorrhage. (A) Total adventitial mast cells content of vehicle and DNP challenged animals which both had received the mast cell stabilizer cromolyn during challenge (left panel). Frequency of mast cell degranulation in the adventitia of control and DNP challenged plaques was normalized after cromolyn treatment (right panel). (B) No hemorrhage or related phenomena were observed in plaques from vehicle and DNP challenged mice, which had been treated with cromolyn during challenge; likewise no Perl´s iron positive lesions were detected in lesions from cromolyn treated mice.

Discussion

Inflammatory cells have been found to contribute significantly to plaque erosion or rupture, and thus to unstable angina and myocardial infarction[2,4-6]. Illustratively, activated mast cells have been identified in the adventitia of vulnerable and ruptured lesions and their number was found to correlate with the incidence of plaque rupture and erosion[15]. To date it remains to be clarified whether these adventitial mast cells are instrumental in or attracted secondary to plaque rupture. To address this key question, we recruited mast cells to the adventitia of atherosclerotic carotid artery lesions in $ApoE^{-/-}$ mice by eliciting a local delayed type hypersensitivity (DTH) reaction[19], which induces an inflammatory response at the site of provocation, represented by mast cell activation and cellular infiltration.
Indeed, no differences in plasma TNFα and systemic mast cell protease levels were found between vehicle control and DNP challenged animals, suggesting that the local DTH reaction did not elicit a systemic activation of

mast cells but was confined to the site of challenge. While the plaque morphometry remained unaffected, the DNP challenge led to a striking and acute increase in the incidence of intraplaque hemorrhage within three days after challenge, which was confirmed by Perl´s iron staining. Also, iron deposits were observed in the media of these lesions, suggesting that the intimal phenomena likely were elicited in the adventitia and penetrated the media of the plaques. Lesions with intraplaque hemorrhage tended to contain relatively more adventitial mast cells than lesions lacking hemorrhages, which is in line with the observation of Laine *et al*.[15], that the adventitia of ruptured lesions in human coronary artery species contained increased levels of mast cells. Importantly, the total numbers of mast cells detected in adventitia of mouse carotid artery plaques after challenge corresponded with those observed in adventitial tissue of human plaques[15,16], indicating that the mouse model offers a realistic representation of the human situation. Intraplaque hemorrhage seemed to colocalize with ceroid-rich regions in close proximity of microvessels and was confined mostly to the central atheroma. Mast cells were reported to induce apoptosis of not only cardiomyocytes[26], but also vascular smooth muscle cells[11,31] and endothelial cells[32] *in vitro*, which might result in reduced plaque stability[35,36]. TUNEL staining of the plaques indeed revealed a highly significant increase of intimal apoptotic nuclei in the DNP challenged mice. To our surprise, apoptosis was mainly localized in the central atheroma as well, implying that the majority of apoptotic cells are of macrophage rather than of vSMC origin. This is in line with the *in vivo* observation that the cap thickness was not influenced by DNP challenge (data not shown). To date, mast cell degranulation has not been linked to macrophage apoptosis. Macrophage apoptosis may very well result in an enlarged necrotic core of the lesions and in the release of tissue factor (TF) rich apoptotic micro-bodies[37], thereby decreasing plaque stability and promoting thrombosis. Our *in vivo* findings concurred with the *in vitro* data, which showed an increased susceptibility of macrophages to mast cell degranulate induced apoptosis, while vascular smooth muscle cells appeared to be less sensitive. Chymase (SBTI) and tryptase (leupeptin) inhibitors were able to prevent macrophage apoptosis induced by the supernatant of degranulated mast cells. Surprisingly, also the H_1-receptor antagonist triprolidine could completely blunt macrophage apoptosis to control levels. Both tryptase and chymase were suggested to be pro-apoptotic by themselves[31], but also to potentiate the pro-apoptotic action of histamine, which was recently shown to act partly via an H_1-receptor dependent mechanism[38]. As our *in vitro* data indicate, histamine indeed acts pro-apoptotic but also appears to sensitize to tryptase induced macrophage apoptosis, whereas tryptase pretreatment did not aggravate histamine induced apoptosis. Tryptase was only able to induce apoptosis of macrophages after prolonged incubation. These data suggest that histamine sensitizes macrophages to tryptase induced apoptosis and promotes apoptosis on its own account possibly by affecting AKT phosphorylation.

Obviously, DNP challenge substantially increased the influx of erythrocytes into the intima of the lesions. We demonstrate here that mast cell degranulation enhances microvascular leakage (a suggested mechanism is depicted in Figure 5E). Indeed, circulating leukocytes were seen to extravasate through mast cell-permeabilized microvessels in response to mast cell derived chemotactic stimuli as shown by the influx of Rhodamine labelled leukocytes into the plaques, leading to an increased presence of inflammatory cells in direct proximity of these vessels. Upon degranulation of adventitial mast cells, the increased microvessel leakage, the pro-inflammatory response and the locally induced apoptosis will act in concert to increase the risk of intraplaque hemorrhage. The increased vascular permeability after exposure to mast cell degranulates was found to be predominantly mediated by histamine in an H_1-receptor dependent manner and to a much lesser extent by mast cell chymase[33] and tryptase[34]. An intriguing question is whether intraplaque hemorrhage per se is an adverse phenomenon or whether it represents a beneficial first step in the wound healing response. Interestingly, Kolodgie *et al*.[39] recently reported that intraplaque hemorrhage is a potent pro-atherogenic stimulus and risk factor in plaque destabilization, as it is accompanied by deposition of erythrocyte associated cholesterol and enlargement of the necrotic core of the atherosclerotic plaque. This concurs with findings described by Kockx *et al*.[40], that phagocytosis of accumulated erythrocytes by activated macrophages leads to ceroid production and further plaque expansion, which may promote the formation of rupture prone lesions.

Treatment of mice with the mast cell stabilizer cromolyn during DNP challenge normalized the extent of mast cell degranulation in the adventitia and of macrophage apoptosis in the central core region of the plaques, while preventing intraplaque hemorrhage. This implies that inhibition of mast cell degranulation in the adventitia of atherosclerotic lesions may help to maintain plaque stability. In some studies, the anti-allergic drug tranilast, which amongst others inhibits mast cell degranulation, was able to suppress atherosclerotic lesion development[41-43], but these results have not been reproduced in human studies[44]. In our study, we used cromolyn, which is a more specific mast cell stabilizer and the observed beneficial effects can thus be fully ascribed to mast cell stabilization.

In conclusion, degranulation of adventitial mast cells did promote macrophage apoptosis and enhanced microvascular leakage in atherosclerotic plaques, resulting in a sharply increased risk of intraplaque hemorrhage. Our findings point to a significant role for activated mast cells in plaque stability and acute coronary syndromes. We propose that mast cell stabilization is an effective new therapeutic entry in the prevention of acute coronary syndromes for patients with unstable angina.

Acknowledgments

The authors would like to thank Dr. Kraneveld and M. Kool from the Utrecht Institute for Pharmaceutical Sciences for assisting with the mMCP ELISA and R. Eggers from the Netherlands Institute for Brain Research in Amsterdam for technical assistance.

References

1. Ross R. Atherosclerosis, an inflammatory disease. *New Engl J Med*. 1999;340:115-126.
2. Shah PK. Mechanisms of plaque vulnerability and rupture. *J Am Coll Cardiol*. 2003;41:15S-22S.
3. Falk E. Why do plaques rupture? *Circulation*. 1992;86:III30-III42.
4. Libby P. Current concepts of the pathogenesis of the acute coronary syndromes. *Circulation*. 2001;104:365-372.
5. Buja LM, Willerson JT. Role of inflammation in coronary plaque disruption. *Circulation*. 1994;89:503-505.
6. Libby P. Inflammation in atherosclerosis. *Nature*. 2002;420:868-874.
7. Kelly JL, Chi DS, Abou-Auda W, Smith JK, Krishnaswamy G. The molecular role of mast cells in atherosclerotic cardiovascular disease. *Mol Med Today*. 2000;6:304-308.
8. Kaartinen M, Penttilä A, Kovanen PT. Accumulation of activated mast cells in the shoulder region of human coronary atheroma, the predilection site of atheromatous rupture. *Circulation*. 1994;90:1669-1678.
9. Kovanen PT, Kaartinen M, Paavonen T. Infiltrates of activated mast cells at the site of coronary atheromatous erosion or rupture in myocardial infarction. *Circulation*. 1995;92:1084-1088.
10. Johnson JL, Jackson CL, Angelini GD, George SJ. Activation of matrix-degrading metalloproteinases by mast cell proteases in atherosclerotic plaques. *Arterioscler Thromb Vasc Biol* 1998;18:1707-1715.
11. Leskinen MJ, Wang Y, Leszczynski D, Lindstedt KA, Kovanen PT. Mast cell chymase induces apoptosis of vascular smooth muscle cells. *Arterioscler Thromb Vasc Biol*. 2001;21:516-522.
12. Kaartinen M, van der Wal AC, van der Loos CM, Piek JJ, Koch KT, Becker AE, Kovanen PT. Mast cell infiltration in acute coronary syndromes: implications for plaque rupture. *J Am Coll Cardiol*. 1998;32:606-612.
13. Kaartinen M, Penttilä A, Kovanen PT. Mast cells in rupture-prone areas of human coronary atheromas produce and store TNFα. *Circulation*. 1996;94:2787-2792.
14. Moreno PR, Purushothaman KR, Fuster V, O'Connor WN. Intimomedial interface damage and adventitial inflammation is increased beneath disrupted atherosclerosis in the aorta: implications for plaque vulnerability. *Circulation*. 2002;105:2504-2511.
15. Laine P, Kaartinen M, Penttilä A, Panula P, Paavonen T, Kovanen PT. Association between myocardial infarction and the mast cells in the adventitia of the infarct-related coronary artery. *Circulation*. 1999;99:361-369.
16. Laine P, Naukkarinen A, Heikkilä L, Pentillä A, Kovanen PT. Adventitial mast cells connect with sensory nerve fibers in atherosclerotic coronary segments. *Circulation*. 2002;101:1665-1669.
17. Chaldakov GN, Stankulov IS, Fiore M, Ghenev PI, Aloe L. Nerve growth factor levels and mast cell distribution in human coronary atherosclerosis. *Atherosclerosis*. 2002;159:57-66.
18. von der Thüsen JH, van Berkel TJC, Biessen EAL. Induction of rapid atherogenesis by perivascular carotid collar placement in apolipoprotein E-deficient and low-density lipoprotein receptor-deficient mice. *Circulation*. 2002;103:1164-1170.
19. Kraneveld AD, Buckley TL, van Heuven-Nolsen D, van Schaik Y, Koster AS, Nijkamp FP. Delayed-type hypersensitivity-induced increase in vascular permeability in the mouse small intestine: inhibition by depletion of sensory neuropeptides and NK1 receptor blockade. *Br J Pharmacol*. 1995;114:1483-1489.

20. Eriksson EE, Werr J, Guo Y, Thoren P, Lindbom L. Direct observations in vivo on the role of endothelial selectins and alpha(4) integrin in cytokine-induced leukocyte-endothelium interactions in the mouse aorta. *Circ Res*. 2000;86:526-533.
21. Kaszaki J, Boros M, Szabo A, Nagy S. Role of histamine in the intestinal flow response following mesenteric ischemia. *Shock*. 1994;2:413-420.
22. Huang M, Pang X, Karalis K, Theoharides TC. Stress-induced interleukin-6 release in mice is mast cell-dependent and more pronounced in apolipoprotein E knock-out mice. *Cardiovasc Res*. 2003;59:241-249.
23. Imlach W, McCaughan CA, Mercer AA, Haig D, Fleming SB. Orf virus-encoded interleukin-10 stimulates the proliferation of murine mast cells and inhibits cytokine synthesis in murine peritoneal macrophages. *J Gen Virol*. 2002;83:1049-1058.
24. Michon IN, Hauer AD, von der Thusen JH, Molenaar TJ, van Berkel TJC, Biessen EA, Kuiper J. Targeting of peptides to restenotic vascular smooth muscle cells using phage display in vitro and in vivo. *Biochim Biophys Acta*. 2002;1591:87-97.
25. He SH, Chen P, Chen HQ. Modulation of enzymatic activity of human mast cell tryptase and chymase by protease inhibitors. *Acta Pharmacol Sin*. 2003;24:923-929.
26. Hara M, Matsumori A, Ono K, Kido H, Hwang MW, Miyamoto T, Iwasaki A, Okada M, Nakatani K, Sasayama S. Mast cells cause apoptosis of cardiomyocytes and proliferation of other intramyocardial cells in vitro. *Circulation*. 1999;100:1443-1449.
27. Lisman T, Leebeek FW, Mosnier LO, Bouma BN, Meijers JC, Janssen HL, Nieuwenhuis HK, De Groot PG. Thrombin-activatable fibrinolysis inhibitor deficiency in cirrhosis is not associated with increased plasma fibrinolysis. *Gastroenterology*. 2001;121:131-139.
28. Sirois ES, Jancar S, Braquet P, Plante GE, Sirois P. PAF increases vascular permeability in selected tissue: effect of BN-52021 and L-655,240. *Prostaglandines*. 1988;36:631-644.
29. Walls AF, Suckling AJ, Rumsby MG. IgG Subclass responses and immediate skin sensitivity in guinea-pigs with chronic relapsing experimental allergic encephalomyelitis. *Int Arch Allergy Appl. Immunol*. 1987;84:109-115.
30. Nakano T, Sonoda T, Hayashi C, Yamatodani A, Kanayama Y, Yamamura T, Asai H, Yonezawa T, Kitamura Y, Galli SJ. Fate of bone marrow-derived cultured mast cells after intracutaneous, intraperitoneal, and intravenous transfer into genetically mast cell-deficient W/Wv mice. Evidence that cultured mast cells can give rise to both connective tissue type and mucosal mast cells. *J Exp Med*. 1985;162:1025-1043.
31. Leskinen MJ, Lindstedt KA, Wang Y, Kovanen PT. Mast cell chymase induces smooth muscle cell apoptosis by a mechanism involving fibronectin degradation and disruption of focal adhesions. *Arterioscler Thromb Vasc Biol*. 2003;23:238-243.
32. Lätti S, Leskinen M, Shiota N, Wang Y, Kovanen PT, Lindstedt KA. Mast cell-mediated apoptosis of endothelial cells in vitro: a paracrine mechanism involving TNFα-mediated down-regulation of blc-2 expression. *J Cell Phys*. 2003;195:130-138.
33. He S, Walls AF. The induction of a prolonged increase in microvascular permeability by human mast cell chymase. *Eur J Pharmacol*. 1998;352:91-98.
34. He S, Walls AF. Human mast cell tryptase: a stimulus of microvascular leakage and mast cell activation. *Eur J Pharmacol*. 1997;328:89-97.
35. von der Thüsen JH, van Vlijmen BJ, Hoeben RC, Kockx MM, Havekes LM, van Berkel TJC, Biessen EA. Induction of atherosclerotic plaque rupture in apolipoprotein E-/- mice after adenovirus-mediated transfer of p53. *Circulation*. 2002;105:2064-2070.
36. Bennett MR. Apoptosis in the cardiovascular system. *Heart*. 2002;87:480-487.
37. Hutter R, Valdiviezo C, Sauter BV, Savontaus M, Chereshnev I, Carrick FE, Bauriedel G, Luderitz B, Fallon JT, Fuster V, Badimon JJ. Caspase-3 and tissue factor expression in lipid-rich plaque macrophages: evidence for apoptosis as link between inflammation and atherothrombosis. *Circulation*. 2004;109:2001-2008.
38. Hur J, Kang MK, Park JY, Lee SY, Bae YS, Lee SH, Park YM, Kwak JY. Pro-apoptotic effect of high concentrations of histamine on human neutrophils. *Int Immunopharmacol*. 2003;3:1491-1502.
39. Kolodgie FD, Gold HK, Burke AP, Fowler DR, Kruth HS, Weber DK, Farb A, Guerrero LJ, Hayase M, Kutys R, Narula J, Finn AV, Virmani R. Intraplaque hemorrhage and progression of coronary atheroma. *N Engl J Med*. 2003;349:2316-2325.

40. Kockx MM, Cromheeke KM, Knaapen MW, Bosmans JM, De Meyer GR, Herman AG, Bult H. Phagocytosis and macrophage activation associated with hemorrhagic microvessels in human atherosclerosis. *Arterioscler Thromb Vasc Biol*. 2003;23:440-446.
41. Matsumura T, Kugiyama K, Sugiyama S, Ota Y, Doi H, Ogata N, Oka H, Yasue H. Suppression of atherosclerotic development in wanatabe heritable hyperlipidemic rabbits treated with an oral anti-allergic drug, tranilast. *Circulation*. 1999;99:919-924.
42. Shiota N, Okunishi H, Takai S, Mikoshiba I, Sakonjo H, Shibata N, Miyazaki M. Tranilast suppresses vascular chymase expression and neointima formation in balloon–injured dog carotid artery. *Circulation*. 1999;99:1084-1090.
43. Saiura A, Sata M, Hirata Y, Nagai R, Makuuchi M. Tranilast inhibits transplant-associated coronary arteriosclerosis in a murine model of cardiac transplant. *Eur J Pharm*. 2001;433:163-168.
44. Holmes DR, Savage M, LaBlanche JM, Grip L, Serruys PW, Fitzgerald P, Fischman D, Goldberg S, Brinker JA, Zeiher AM, Shapiro LM, Willerson J, Davis BR, Ferguson JJ, Popma J, King SB, Lincoff AM, Tcheng JE, Chan R, Granett JR, Poland M. Results of prevention of restenosis with tranilast and its outcomes (PRESTO) trial. *Circulation*. 2002;106:1243-1250.